THE ASTROPHYSICAL JOURNAL, 417:738–741, 1993 November 10

GAMMA-RAY AND RADIO OBSERVATIONS OF PSR B1509−58

M. P. ULMER,[1] S. M. MATZ,[1] R. B. WILSON,[2] M. J. FINGER,[2,3] K. S. HAGEDON,[2,4] D. A. GRABELSKY,[1]
J. E. GROVE,[5,6] W. N. JOHNSON,[5] R. L. KINZER,[5] J. D. KURFESS,[5] W. R. PURCELL,[1]
M. S. STRICKMAN,[5] V. M. KASPI,[7] S. JOHNSTON,[8] R. N. MANCHESTER,[7]
A. G. LYNE,[9] AND N. D'AMICO[10]
Received 1993 March 22; accepted 1993 May 17

ABSTRACT

We report concurrent radio and gamma-ray observations of PSR B1509−58 carried out by the Parkes Radio Telescope and by the Burst and Transient Source Experiment (BATSE) and the Oriented Scintillation Spectrometer Experiment (OSSE) on the *Compton Gamma-Ray Observatory* (*CGRO*). Gamma-ray light curves fitted at several energies between ∼20 and 500 keV yield a phase offset with respect to the radio pulse that is independent of energy, with an average value 0.32 ± 0.02. Although this value is larger by 0.07 than that reported by Kawai et al., the difference is not statistically significant (only $\sim 2\ \sigma$) when account is taken of the uncertainty associated with their result. We briefly discuss the possibility that the energy independence of the gamma-ray pulse phase is a signature of nonthermal radiation in the X-ray/gamma-ray range and the suggestion of a dependence of pulsar radio–gamma-ray phase offset on pulse period.

Subject headings: gamma rays: observations — pulsars: individual (PSR B1509−58) — radio continuum: stars

1. INTRODUCTION

Until recently there were only two radio pulsars, the Crab and Vela, which had also been detected in hard X-rays/gamma-rays, and they differed both in spectral shape and in the behavior of the pulse phase as a function of energy. The Crab pulsar spectrum can be fitted by a power law in the ∼1–200 keV energy range (Knight 1982, 1983, and references therein; Ulmer et al. 1993). The double-peaked pulse is aligned in phase at all frequencies from the radio to the gamma rays. On the other hand, the Vela pulsar X-ray spectrum in the 0.1–2.4 keV range is probably of thermal origin (Ögelman, Finley, & Zimmerman 1993), and the phases of the Vela pulsar peaks shift from the optical to X-rays to gamma rays (Ögelman et al. 1993; Manchester & Taylor 1977, hereafter MT77; Lyne & Graham-Smith 1990, hereafter LGS 90).

Instruments on the *Compton Gamma-Ray Observatory* (*CGRO*) have now detected three additional radio pulsars: PSR B1706−44, PSR B1055−52, and PSR B1509−58 (Thompson et al. 1992; Fierro et al. 1993; Wilson et al. 1992b). OSSE and BATSE have not yet detected PSR B1706−44 and PSR B1055−52 at hard X-ray energies, but we have seen PSR B1509−58. Like the Crab, it has a nonthermal, power-law spectrum from the soft to hard X-rays (Seward & Harnden 1982; Seward, Harnden, & Elsner 1985; Wilson et al. 1992b; Wilson et al. 1993; Matz et al. 1993). However, unlike the Crab pulsar, the radio pulse phase differs markedly (∼0.3) from the phase of the soft X-ray (2–11 keV) peak (Kawai et al. 1991, hereafter K91).

In this paper we report on pulse phase observations of PSR B1509−58 which combine data from the BATSE (Wilson et al. 1992a) and OSSE (Johnson et al. 1993) experiments on *CGRO*, covering ∼20–500 keV in energy, along with nearly contemporaneous ∼2 GHz radio observations made at the Parkes Radio Telescope. By comparing the hard X-ray and radio pulse phases we can verify the phase shift measured by *Ginga* (K91) and determine whether the pulse varies over two orders of magnitude in photon energy. We describe the observations and analysis procedures in § 2 and present our results for PSR B1509−58 in § 3. In § 4 we briefly discuss our results in comparison with other pulsars.

2. OBSERVATIONS AND ANALYSIS

2.1. *Radio Observations and Ephemeris*

The radio observations of PSR B1509−58 were made at the Parkes Radio Telescope over regular intervals during the period MJD 47931−48896, using two observing systems centered at frequencies of 1.52 and 2.36 GHz. Details of the observing apparatus and procedures are given in K91. To maintain consistency when comparing results, we adopt their dispersion measure (DM) of 253 ± 1 cm^{-3} pc, derived by comparing the average pulse profiles at the two observed frequencies. Using these radio data we derived an ephemeris for this pulsar; the parameters are given in Table 1, where ν, $\dot{\nu}$, and $\ddot{\nu}$ are the pulsar frequency and its first and second derivatives.

The radio phase is defined by the UTC geocentric arrival time of a fiducial peak. By convention, the first peak after the beginning of a day near the (temporal) center of the radio observations used to define the ephemeris is chosen; the reference time is referred to as $t_{0_{\rm geo}}$. The ephemeris derived gives the arrival time at the geocenter for an "infinite frequency" pulse,

[1] Department of Physics and Astronomy, Northwestern University, Evanston, IL 60208.
[2] MSFC-ES66, MSFC, AL 35812.
[3] Astronomy Programs, Computer Sciences Corporation.
[4] University Space Research Associates.
[5] Code 7650, NRL, E. O. Hulburt Center for Space Research, Washington, DC 21875.
[6] NRC/NRL Resident Research Associate.
[7] Dept. of Physics, Princeton University, Princeton, NJ 08544.
[8] Australia Telescope National Facility, CSIRO, P.O. Box 76, Epping, NSW 2121, Australia.
[9] Department of Physics, University of Manchester, Jodrell Bank, Macclesfield, SK11 9DL, UK.
[10] Istituto di Fisica dell'Universita di Palermo and Istituto di Radioastronomie del CNR, I-40126 Bologna, Italy.

TABLE 1

RADIO EPHEMERIS FOR PSR B1509−58

ν	6.6371895831124 s^{-1}
$\dot{\nu}$	-6.76844×10^{-11} s^{-2}
$\ddot{\nu}$	1.97×10^{-21} s^{-3}
t_0(TDB)	48420.0
t_{0geo}(MJD)	48420.000000121
R.A. (J2000)	$15^h13^m55^s.667$
Decl. (J2000)	−59°08′9″.42

that is, a radio pulse corrected for DM. To transform from the geocenter to the solar system barycenter (SSB), we employed a version of the standard software package TEMPO (Taylor & Weisberg 1989), in conjunction with the Jet Propulsion Laboratory DE200 solar system ephemeris (epoch J2000), kindly provided by E. M. Standish (1989, private communication). The best-fit position of PSR B1509−58 used for this solution is shown in Table 1. The epoch range for which this solution was derived is MJD 47913−48928.

2.2. *BATSE and OSSE Analysis*

The BATSE and OSSE instruments are described in detail in Fishman et al. (1989) and Johnson et al. (1993). Here we briefly describe the timing data that we analyzed for this paper. For both instruments, the data were accumulated in relatively broad energy channels chosen prior to the observation. We report here data from three OSSE and seven BATSE energy bands, covering ~20–480 keV.

The BATSE data from the source-facing detectors were accumulated in 64 bin phase histograms on board, obtained by folding the data over an integral number of "mean" pulse periods for a programmable duration, normally 8.0 s. For 27% of the exposure reported here, durations of 130 s have been used. The hardware performs the function of a multichannel scaler, successively stepping to the adjacent phase bin every 1/64th of the folding period. Detected counts are accumulated into the currently active phase bin, based on their UTC arrival times at the spacecraft. The period used for this on-board processing was the mean observed period in the reference frame of the spacecraft, specified to the nearest microsecond. The period used includes the effects of the Earth's motion relative to the source; a single value for the period is used throughout the *CGRO* orbit. The maximum mean phase drift occurring over either integration time is less than 0.5 phase bins. Data are recorded separately for each of 16 energy channels. These data, along with the starting time of the accumulation as measured by a simultaneous latch of the *CGRO* spacecraft clock, read out with a precision of 1/64 ms, are telemetered to the ground.

In ground processing, the SSB arrival time of the 65 bin edges nearest to the midpoint of the accumulation are computed, using software derived from TEMPO with the JPL DE200 solar system ephemeris and the pulsar radio position given in Table 1. The counts are then summed into 64 phase bins fixed in the SSB, splitting counts linearly into adjacent bins based on the relative overlap with the SSB bins.

The OSSE pulsar data for PSR B1509−58 were accumulated as rates in 8 ms time intervals; each sample is tagged with its UTC arrival time at the spacecraft. After transmission to the ground, UTC times were corrected to the solar system barycenter using the same software as BATSE, then epoch-folded using the radio ephemeris. During the OSSE observation, two detectors were continuously pointed at the pulsar and two alternated source and background pointings every 2 minutes. Pulsar data were only collected from a detector when it was pointing at the source.

We have taken considerable care to ensure that both BATSE and OSSE (in fact, all *CGRO* instruments) use consistent pulsar analysis techniques (including as much common software as possible), and have verified the consistency of our results by comparing light curves of the Crab pulsar.

For both instruments, the epoch-folding procedure computed the phase (ϕ) of the pulsar according to the formula

$$\phi(t) = \phi(t_0) + \nu_0(t - t_0) + \dot{\nu}_0(t - t_0)^2/2 + \ddot{\nu}_0(t - t_0)^3/6 \,. \quad (1)$$

The radio ephemeris for PSR B1509−08, including the parameters of this formula, are given in Table 1.

2.3. *CGRO Timing Accuracy and Stability*

The rated stability and accuracy of the satellite clock and the accuracy of the satellite position information combine to give an expected absolute timing accuracy of 100 μs. We have used observations of the Crab pulsar to verify this value by measuring the absolute timing accuracy and the long-term clock drift. The stability of the clock is important to our analysis because the BATSE observations of PSR B1509−58 cover a much longer period of time than those of OSSE (MJD 48561−48920 for BATSE vs. MJD 48910−48924 for OSSE).

The absolute accuracy of the *CGRO* clock was demonstrated by epoch-folding the OSSE Crab pulsar data using the radio ephemeris of Arzoumanian, Nice, & Taylor (1992). The primary peaks of the gamma-ray and radio pulses agreed to better than ~0.3 ms, the typical absolute accuracy limit for radio pulsar observations. We conclude that absolute accuracy of *CGRO* timing data is at least this good.

Limits on clock drift were determined by OSSE using light curves produced from Crab observations separated by 3 weeks; the data were accumulated over periods of one day to 1 week. Comparison among these various light curves showed no change to better than 0.01 in phase over $\sim 6 \times 10^8$ cycles, demonstrating that any drift in the *CGRO* clock was negligible. BATSE has observed the Crab pulsar continuously since the launch of *CGRO*. Using the ephemerides of Arzoumanian et al. (1992), with the assumption that any observed change in arrival phase of the observed gamma-ray pulse profile is due to errors in the *CGRO* clock, a limit of $^{+0.3}_{-0.5}$ ms can be placed on the drift of the clock throughout the *CGRO* mission ($^{+0.3}_{-0.2}$ ms during the observations of PSR B1509−58 reported here).

Therefore both the absolute accuracy and drift uncertainties in the *CGRO* clock, determined independently by the OSSE and BATSE measurements of the Crab pulsar, are on the order of 0.3–0.5 ms. Uncertainties of this magnitude are small (~0.3%) compared to the 150 ms period of the PSR B1509−58 and the X-ray/radio phase shift, and are comparable to the statistical errors for the combined BATSE and OSSE data (see § 3).

3. RESULTS

In Figure 1 we show the results of the analysis described above in the form of three average light curves: the radio data, the 20–50 keV BATSE data, and the best signal-to-noise light curve for higher energies (50–170 keV) from OSSE. Light curves in all the *CGRO* energy bands will be reported elsewhere (Wilson et al. 1993; Matz et al. 1993).

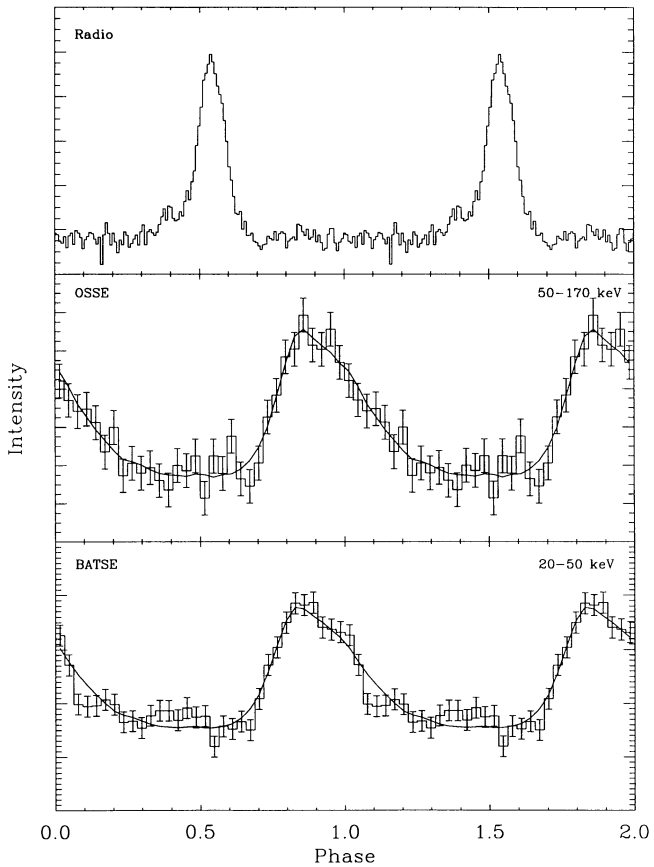

FIG. 1.—Three average light curves. The smooth curve on the lower two plots is the average light curve from K91, normalized and shifted to fit the *CGRO* data.

Although the pulsed emission is clearly significant in both gamma-ray light curves, the statistical fluctuations from bin to bin are large enough that we cannot accurately measure the phase of the peaks directly from the data. Instead, we have fitted the observed light curves with a model pulse profile in order to determine the phase of the gamma-ray peak. We used two approaches: The first was to fit the gamma-ray light curves with a Gaussian peak plus a constant amplitude offset. Applied to the light curves shown in Figure 1, this method yielded a relative gamma-ray phase of 0.36 ± 0.01. The χ^2 for the fits were 72 and 59 for BATSE and OSSE, respectively, for 60 degrees of freedom.

Although these χ^2 values indicate statistically acceptable fits to the data, the Gaussian model does not reflect the apparent asymmetry of the light curve. For this reason we applied a second model, using the 32 phase bin $\sim$2–11 keV *Ginga* light curve (K91) as a template to fit the *CGRO* light curves. The free parameters for this fit were the phase and normalization of the template plus a constant DC count level. Model values for phase shifts of a fraction of a phase bin were determined by linearly interpolating between adjacent bins in the *Ginga* light curve.

For the light curves in Figure 1, the best fit required a shift in the previously reported phase of the K91 light curve, relative to the peak in the radio light curve, of 0.07 ± 0.02. Note that because we have used the K91 light curve as a template, their relative phase of 0.25 is treated as a reference phase for the template, with no associated uncertainty. The implied relative phase of the gamma-ray peak from the OSSE and BATSE data is then 0.32 ± 0.02. For 61 degrees of freedom, we obtained a χ^2 of 84 and 53 for BATSE and OSSE, respectively. Thus this model is also a statistically acceptable description of the data, which implies that there is no evidence for a change in the light curve shape from the soft to hard X-rays.

To measure the energy dependence of the pulse phase we have accumulated light curves from BATSE and OSSE over seven and three broad energy ranges, respectively, covering the energy range $\sim$20–500 keV. Then at each energy the best-fit phase-shift values were determined using the *Ginga* light curve as a fitting template. The results are displayed in Figure 2.

The weighted-average phase shift determined from the combined OSSE and BATSE points (Fig. 2) is 0.315 ± 0.005. The uncertainty on this result approaches the accuracy of the radio data; it is purely statistical, however, and does not include the inherent resolution of the model light curve (about 0.016 in phase) or uncertainties in the *CGRO* clock ($\sim$0.003) or radio peak position ($\sim$0.003). Taking these sources of error into account, we quote our best value for the phase shift as 0.32 ± 0.02. Separate fits to subintervals of the BATSE observations are consistent with no time evolution of this offset.

4. DISCUSSION

The peak of the gamma-ray pulse of PSR B1509−58 is clearly offset in phase from the peak in the radio. Our gamma-ray light curves cover $\sim$20–480 keV in energy, compared with $\sim$2–11 keV for the K91 measurement. When proper account is taken of the revised uncertainties in the *Ginga* position, their phase offset relative to the radio is 0.25 ± 0.03 (K91 and N. Kawai 1992, private communication). The adjustment of 0.07 ± 0.02 that we have determined to this phase offset is therefore only marginally significant ($\sim 2\ \sigma$). It is clear from Figure 2 that there is no significant variation with energy over the $\sim$20–500 keV energy range spanned by the *CGRO* data. Evidently then, PSR B1509−58 is like the Crab pulsar (cf. LGS90; MT77) in this respect. Unlike the Crab pulsar however, with its very small X-ray/radio phase offset ($\sim$0.05 or $\lesssim$ 0.01, depending on whether the precursor or the main

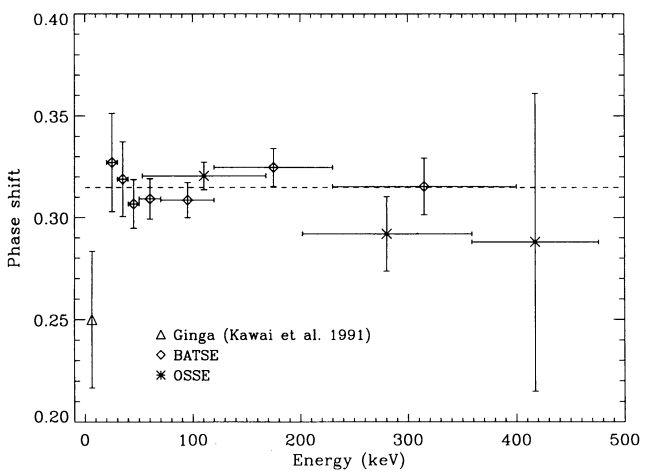

FIG. 2.—Best-fit phases (with respect to the radio peak) of the *CGRO* pulses as a function of energy. The K91 light curve was used as the template for determining the phase. *Triangle*: data point from K91; *asterisks*: OSSE data; *diamonds*: BATSE data. *Dashed line*: weighted average of all the points. *Horizontal bars*: energy ranges over which the fitted light curves were accumulated.

pulses are used to define the radio reference phase; see, e.g., MT77 and LGS90), the relative phase offset observed for PSR B1509−58 is fairly large.

It is difficult to make a detailed comparison of this result with the gamma-ray and radio pulsars PSR B1706−44 and PSR B1055−52 (Thompson et al. 1992; Fierro et al. 1993) because their gamma-ray signals are weak and their pulse shapes are not well determined. It does appear, however, that the gamma-ray peaks of these pulsars are also not aligned with the radio peaks. Since this is also the case for the Vela pulsar (LGS90; MT77), in this respect, at least, the Crab is the "unusual" object in the set of *CGRO*-detected radio pulsars.

We note (as K91 noted) that in progressing from the Crab to PSR B1509−58 the period and the radio/gamma-ray phase offset seem to increase together. There are a number of difficulties, however, which make this apparent correlation problematic. It is not obvious how to construct a meaningful definition of phase shift which can be uniformly applied to pulsars with markedly different pulse shapes. In addition, there is an inherent ambiguity in calculating the phase difference: do the gamma-rays lag the radio by ϕ, or lead by $1-\phi$? We ignore these difficulties because the limited data do not warrant a detailed study here (see Ulmer 1993 for further discussion). We will remark that the trend of increasing offset with increasing period predicts that fast (periods $\simeq 50$ ms) pulsars which have X-ray emission dominated by nonthermal processes such as PSR B0540−69 (Seward, Harnden, & Helfand 1984; Finley et al. 1993) will have a small ($\lesssim 0.1$) radio/gamma-ray phase offset. It will be interesting therefore to make simultaneous X-ray/optical and radio observations of pulsars such as PSR B0540−69.

Because the spectra of PSR B1509−58 from ~ 0.5 to 3.5 keV (Seward & Harnden 1982; Seward et al. 1985) and from ~ 20 to 200 keV (Wilson et al. 1993; Matz et al. 1993) appear to be well described by power laws with similar spectral indices, the X-ray and gamma-ray emission is probably nonthermal in origin. Based on the apparent energy independence of the peak phase of the X-ray/hard gamma-ray light curves of PSR B1509−58 and of the Crab pulsar (which also has a power-law spectrum), we suggest that a signature of nonthermal radiation processes is the phase locking of the $\gtrsim 2$ keV emission over a broad ($\gtrsim 400$ keV) energy range. Conversely, the signature of thermal processes is the absence of such phase locking from the soft to the hard X-rays. The Vela pulsar is an example of a source of thermal X-ray emission (Ögelman et al. 1993) and nonthermal gamma-ray emission (Strickman et al. 1993; Kanbach et al. 1980) whose pulse phase varies over this energy range.

We thank the *CGRO* flight operations team lead by B. Breshears for providing us with a stable and accurate clock. We are also grateful to N. Kawai for providing us with his data and comments on the *Ginga* timing, and to J. Arons and A. Harding for useful discussions. We thank D. Thompson and J. Fierro for making their results on PSR B1055−52 available to us prior to publication. This work was supported in part by NASA grant DPR S-10987C.

REFERENCES

Arzoumanian, Z., Nice, D., & Taylor, J. H. 1992, *CGRO*/radio timing data base, Princeton Univ.
Fierro, J. M., et al. 1993, ApJ, 413, L27
Finley, J. P., Ögelman, H., Hasinger, G., & Trümper, J. 1993, ApJ, submitted
Fishman, G. J., et al. 1989, in Proc. GRO Science Workshop (1989 April 10–12), ed. W. N. Johnson (Greenbelt, MD: Goddard Space Flight Center), 2
Johnson, W. N., et al. 1993, ApJS, 86, 693
Kanbach, G., et al. 1980, A&A, 90, 163
Kawai, N., Okayasu, R., Brinkman, W., Manchester, R., Lyne, A. G., & D'Amico, N. 1991, ApJ, 383, L65 (K91)
Knight, F. K. 1982, ApJ, 260, 578
———. 1983, in Positron-Electron Pairs in Astrophysics, ed. M. L. Burns, A. K. Harding, & R. Ramaty (New York: AIP), 141
Lyne, A. G., & Graham-Smith, F. 1990, Pulsar Astronomy (Cambridge: Cambridge Univ. Press) (LGS90)
Manchester, R. N., & Taylor, J. H. 1977, Pulsars (San Francisco: W. H. Freeman and Company) (MT77)
Matz, S. M., et al. 1993, in preparation
Ögelman, H., Finley, J. P., & Zimmerman, H. U. 1993, Nature, 361, 136
Seward, F. D., & Harnden, F. R., Jr. 1982, ApJ, 256, L45
Seward, F. D., Harnden, F. R., Jr., & Elsner, R. F. 1985, in Crab Nebula and Related Supernova Remnants, ed. M. C. Kafatos & R. C. Henry (Cambridge: Cambridge Univ. Press), 165
Seward, F. D., Harnden, F. R., Jr., & Helfand, D. J. 1984, ApJ, 287, L19
Strickman, M. S., et al. 1993, in Proc. First Compton Observatory Symposium (1992 October 15–17), ed. N. Gehrels (New York: AIP), in press
Taylor, J. H., & Weisberg, J. M. 1989, ApJ, 345, 434
Thompson, D. J., et al. 1992, Nature, 359, 615
Ulmer, M. P. 1993, in preparation
Ulmer, M. P., et al. 1993, in Proc. Isolated Pulsar Workshop, ed. K. A. van Ripper, R. Epstein, & C. Ho (Cambridge: Cambridge Univ. Press), 251
Wilson, R. B., Finger, M. H., Fishman, G. J., Meegan, C. A., & Paciesas, W. S. 1992a, in Proc. Isolated Pulsar Workshop, ed. K. A. van Ripper, R. Epstein, & C. Ho (Cambridge: Cambridge Univ. Press), 380
Wilson, R. B., Finger, M. H., Pendleton, G. N., Fishman, G. J., Meegan, C. A., & Paciesas, W. S. 1992b, in Proc. Isolated Pulsar Workshop, ed. K. A. van Ripper, R. Epstein, & C. Ho (Cambridge: Cambridge Univ. Press), 257
Wilson, R. B., et al. 1993, in preparation